Synthesis, Separation, and Characterization of Polymers from Gold Monolayer Protected Clusters

Anthony Stevenson

A thesis submitted to the faculty of the University of North Carolina at Chapel Hill in partial fulfillment of the requirements for the degree of Master of Arts in the Department of Chemistry.

Chapel Hill

2008

Approved by:

Dr. Royce Murray

Dr. Mark Wightman

Dr. James Jorgenson

Abstract

ANTHONY STEVENSON: Synthesis, Separation, and Characterization of Polymers
from Gold Monolayer Protected Clusters
(Under the direction of Dr. Royce Murray)

This work details the advances made in the synthesis, separation, and

characterization of small-chain gold monolayer protected cluster (MPC) polymers.

Particles of 25 gold atoms (exhibiting molecule-like electronic behavior) or 140 gold

atoms (showing electronic properties between those of molecular and bulk gold) were

used to allow investigation of changes to these phenomena with MPC polymer assembly.

Two classes of coupling chemistry, dithiol linkers and carbodiimide ester or amide

formation, have been employed to synthesize these MPC polymers. Matrix assisted laser

desorption ionization mass spectrometry has been used to aid in the identification of

mixed monolayer starting materials, as well as to search for direct evidence of MPC

assemblies. High performance reverse phase liquid chromatography and size exclusion

chromatography have been used to separate complex mixtures of reaction products and

isolate MPC polymers. TEM of these collected fractions has allowed imaging of MPC

polymer assemblies.

Table of Contents

List of Figures

Introduction

Numerous applications have been proposed for the use of gold monolayer protected clusters (MPC's) in sensing and molecular electronics[1-4]. The fundamental concepts of electron transfer between these clusters, however, have not been fully explored. This work details the advances made in the synthesis, separation, and characterization of small-chain MPC polymers to allow further study of the fundamental theory of electron transfer dynamics at fixed distances between cores. Particles of 25 gold atoms (exhibiting molecule-like electronic behavior) or 140 gold atoms (showing electronic properties between those of molecular and bulk gold) were used to allow investigation of changes to these phenomena with MPC polymer assembly. Two classes of coupling chemistry, dithiol linkers and carbodiimide ester or amide formation, have been employed to synthesize these MPC polymers. Matrix assisted laser desorption ionization mass spectrometry has been used to aid in the identification of mixed monolayer starting materials, as well as to search for direct evidence of MPC assemblies. High performance reverse phase liquid chromatography and size exclusion chromatography have been used to separate complex mixtures of reaction products and isolate MPC polymers. TEM of these collected fractions has allowed us to view MPC polymer assemblies.

Monolayer Protected Clusters

A great deal of research in recent years has been devoted to the study of monolayer protected clusters because of their unique size-dependant properties. An MPC may be defined as a nanoparticle consisting of a metallic core encapsulated by a number of covalently-bound stabilizing ligands. This work will confine itself to the study of particles consisting of a gold core protected by organic thiolate ligands.

The distinctive characteristic of interest in the study of these clusters is the variance of optical and electrochemical properties with core size, particularly in clusters smaller than a few hundred atoms. These properties change from resembling bulk gold in larger nanoparticles, including the presence of a surface plasmon as observed with UV-visible spectroscopy, to the observation of a molecule-like HOMO-LUMO gap for smaller MPC's[5-7]. Between these two extremes, a phenomenon known as quantized double layer charging can be seen, whereby the small (sub-attofarad) capacitance created between an electrolyte solution and the metallic core through a non-conducting alkane thiol monolayer allows the observation of single electron charging of the core[8-12].

Analytical and preparative separations of MPC's have been achieved using a number of chromatographic and electrophoretic techniques (depending on monolayer composition), including reverse phase high performance liquid chromatography[13-15], size exclusion chromatography[16-18], ion pair chromatography[19], gel electrophoresis[20,21], and capillary electrophoresis[22-24]. Not all of these techniques, however, are suitable for separation of alkane thiolated MPC's, and while reverse phase high performance liquid

chromatography has shown the most success with these particles, a single definitive

technique for separation of MPC's or MPC polymers with small (<200 gold atom)

clusters has not been shown. This work focuses on separation by size exclusion and

reverse phase high performance liquid chromatography.

The groundwork for MPC synthesis has been laid out in the extensive research

conducted to explore ligand place exchange reactions[25-29]. Additional coupling reactions

have then been performed to covalently link molecules to the ends of substituted alkane

thiol ligands[30]. The majority of MPC coupling chemistry has been focused on the

creation of films[31,32] or scaffolds[33] for larger nanoparticle assemblies. Stellacci et al.

have reported MPC's several nanometers in diameter attached in a linear chain, with each

particle covalently bonded at two diametrically opposed points via an amide bond with

1,6-diaminohexane to another particle[34]. Feldheim et al. have shown dimer, trimer, and

tetramer formation using multi-dentate phenylacetylene bridges to citrate-stabilized

particles[18,35,36].

The MPC molecule most used in this report is $Au_{25}(SCH_2CH_2Ph)_{18}$ (referred to

here as Au_{25}). This particle shows remarkable stability and resistance to etching

techniques compared to many other core sizes of MPC, and has a characteristic step-like

UV-visible absorbance spectrum, simplifying identification of this species. This core

size was first synthesized using glutathione (GSH) ligands, and identified[37,38] as

$Au_{25}(GSH)_{16}$. Many subsequent studies characterized the $Au_{25}(Ligand)_{18}$ species while

erroneously identifying it as $Au_{38}(Ligand)_{24}$. It was only with the application of

electrospray ionization mass spectrometry (ESI-MS) that the $Au_{25}(Ligand)_{18}$ species was

confidently identified[39,40]. Refinement of matrix assisted laser desorption ionization was

later able to show a parent molecular ion peak[41] for $Au_{25}(SCH_2CH_2Ph)_{18}$. Experimentally determined X-ray diffraction crystal structure and theoretical models confirm the Au_{25} assignment, describing a 13-atom icosahedral core protected by 6 RS-Au-RS-Au-RS units[42-44]. The $Au_{38}(Ligand)_{24}$ molecule, however, has also been shown to exist using ESI-MS as a stable product which can be isolated[45].

Synthesis of MPC's and MPC Polymers

Synthesis of Gold Monolayer Protected Clusters:

$Au_{25}(SCH_2CH_2Ph)_{18}$ and $Au_{140}(SC_6H_{12})_{53}$ (referred to here as Au_{140}) were synthesized using a modified Brust synthesis[46]. Aqueous gold chloride ($HAuCl_4$) was transferred into dichloromethane (for Au_{25}) or toluene (for Au_{140}) using tetraoctylammonium bromide as the phase transfer reagent. Phenylethanethiol or hexane thiol, for Au_{25} or Au_{140} respectively, was added to solution with stirring, forming a gold-thiol polymer. Sodium borohydride was added at 0°C and allowed to react for one hour (for Au_{25}) or overnight (for Au_{140}). The sodium borohydride reduces the gold-thiol polymer, beginning a process of growth of the nanoparticle by the formation of gold-gold bonds, and passivation by the formation of gold-thiol bonds. Growth of the nanoparticle stops when it has been fully encapsulated in a thiolate monolayer. Excess phenylethanethiol ligand was removed by washing with methanol, and Au_{25} was purified by extraction into acetonitrile. Au_{140} was extracted into ethanol and further purified using an annealing process, by which excess hexane thiol was added with stirring and removed after several hours.
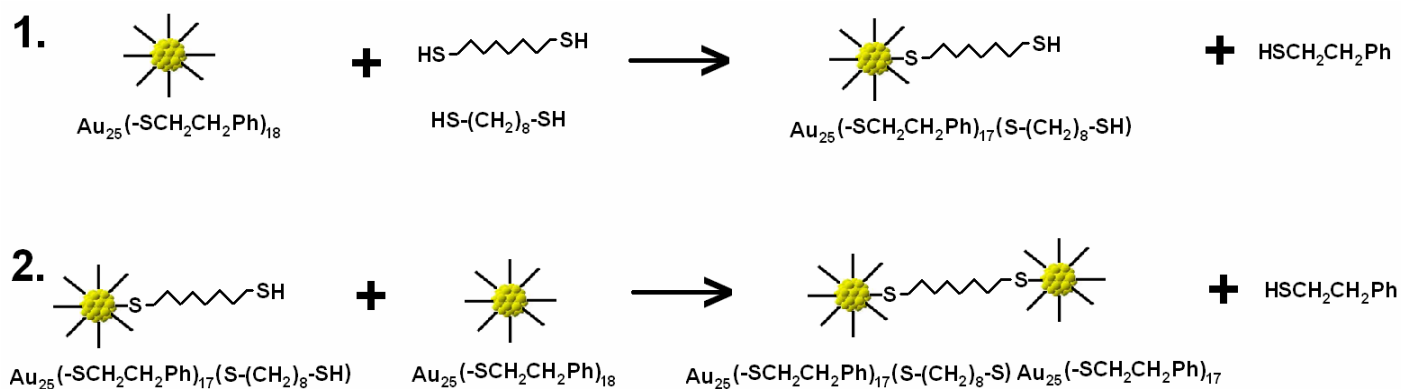
Dithiol MPC Coupling:

Coupling of gold thiolate MPC's was achieved using two classes of linking chemistry – dithiol coupling and carbodiimide coupling. Dithiol coupling bonds two ends of a dithiol directly to the gold core of two different MPC's. Carbodiimide coupling was used to form ester or amide bonds between functionalized sites in the MPC monolayer.

Dithiol coupling involves the use of an alkyl or conjugated dithiol linker. Each thiol group bonds to the gold core of a different MPC, thus linking multiple MPC's together. The extent of dithiol incorporation into the monolayer provides additional linking sites, leading to the formation of dimers, trimers, tetramers, and larger polymers of dithiol-linked MPC's, and defines the limits of polymer length. In order to study coupling of just a few MPC monomers, the number of dithiol units in the monolayer must be kept very low. Even just a few dithiol linking sites in the monolayer could result in very large, insoluble MPC polymers.

A ligand exchange approach was used to replace phenylethanethiol ligand with one thiol end of an incoming dithiol. MPC coupling occurs when the free thiol end of the MPC bound dithiol replaces a second phenylethanethiol ligand on a different MPC. To initiate ligand exchange, the incoming ligand is added to a solution of previously synthesized gold MPC with a different monolayer composition in a small amount of dichloromethane, and stirred for a specified length of time. The extent of ligand exchange depends on the ratio of incoming ligand to core ligands, as well as the reaction

time. MALDI mass spectrometry has shown that the ligand exchange process creates a distribution of the number of ligands exchanged.[41]   Both NMR Spectroscopy and

1.

$Au_{25}(-SCH_2CH_2Ph)_{18}$ + HS$\sim\sim\sim$SH → $Au_{25}(-SCH_2CH_2Ph)_{17}(S-(CH_2)_8-SH)$ + $HSCH_2CH_2Ph$

HS-$(CH_2)_8$-SH

2.

$Au_{25}(-SCH_2CH_2Ph)_{17}(S-(CH_2)_8-SH)$ + $Au_{25}(-SCH_2CH_2Ph)_{18}$ → $Au_{25}(-SCH_2CH_2Ph)_{17}(S-(CH_2)_8-S) Au_{25}(-SCH_2CH_2Ph)_{17}$ + $HSCH_2CH_2Ph$
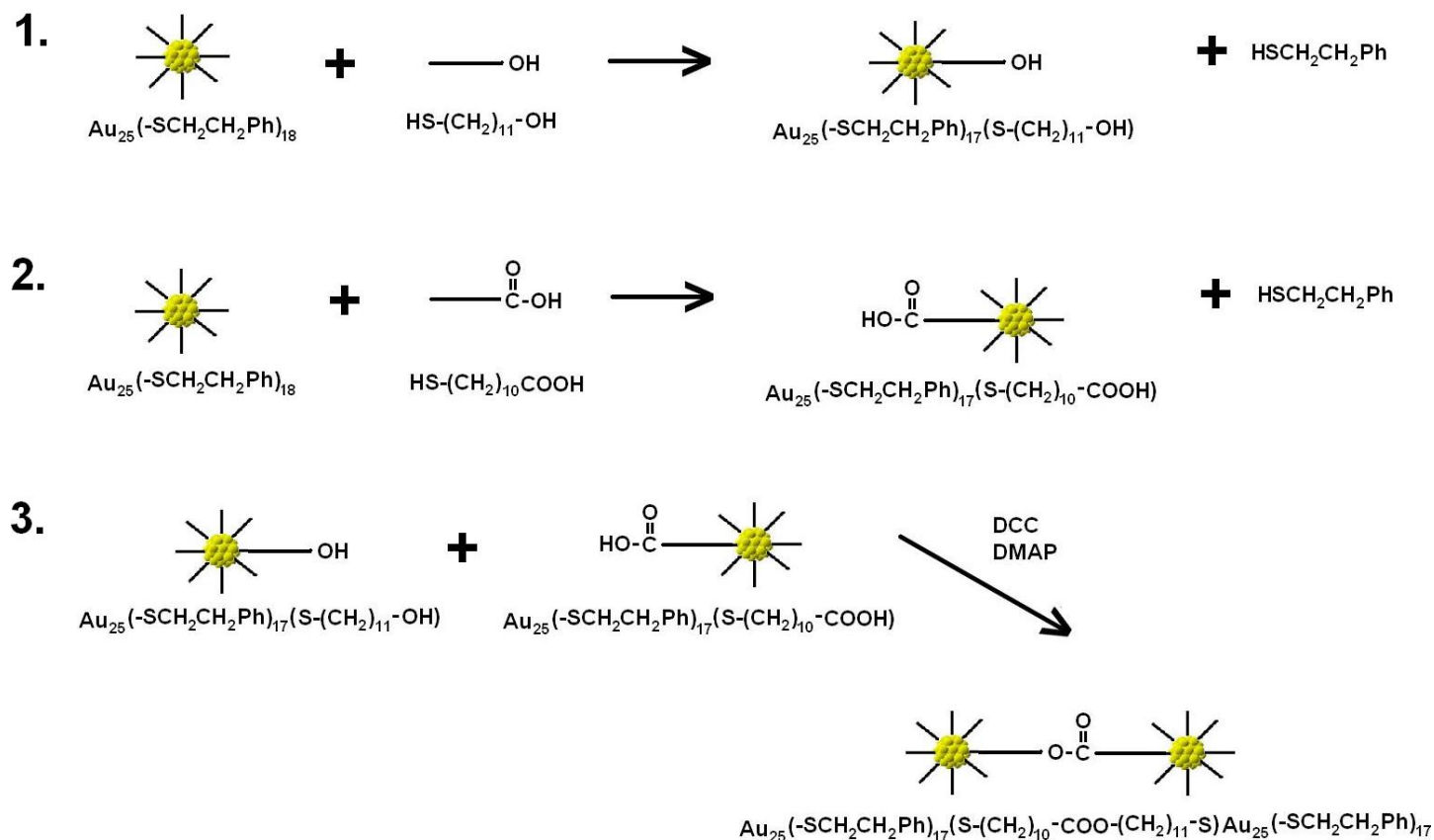
Reaction 1: Dithiol coupling of Au_{25}.

1) Au_{25} undergoes a ligand exchange with octane dithiol. One thiol end of the octane dithiol is incorporated into the monolayer.

2) The free thiol end of the dithiol is incorporated into the monolayer of a different nanoparticle, linking the two particles. Biphenyl dithiol has also been used as a linking molecule.

MALDI-MS have been used to show that the rate of ligand exchange is highly dependent on the chemical structure of the incoming thiol ligand. The ligand exchange process is quenched by removal of the free thiol with a solvent in which the MPC is not soluble. For Au_{25}, methanol and heptane are typically used to remove excess free thiol. The ligand exchange process can also be quenched by chromatographic separation of the free thiol from the MPC.

One challenge present in the dithiol ligand exchange method is the formation of monosubstituted dithiols in the monolayer, resulting in stable, unreacted linking sites. The solution can be analyzed to determine the extent of MPC coupling, but upon reduction of sample volume, the close proximity of monosubstituted dithiols near other MPC monolayers can result in further coupling. This is particularly apparent when previously soluble coupled MPC material forms an insoluble film after rotary evaporation. For this reason, it is imperative to keep the number of dithiol units very low during ligand exchange. Small amounts of dithiol (one dithiol ligand or less per 18 core ligands) reacted over longer times seem to be most effective in creating a stable product.

Carbodiimide MPC Coupling:

A second class of coupling chemistry, carbodiimide coupling, was also used to link MPC's. Carbodiimide molecules are used to activate carboxylic acid functional groups to react with alcohols (to form an ester bond) or amines (to form an amide bond). Three coupling reagents were used; dicyclohexylcarbodiimide (DCC), 1-ethyl-3-(3-dimethylaminopropyl (EDC), and EDC hydrochloride. The MPC monolayers were first modified via ligand exchange with a carboxylic acid thiol, alcohol thiol, or amino thiol

1.

Au$_{25}$(-SCH$_2$CH$_2$Ph)$_{18}$ + HS-(CH$_2$)$_{11}$-OH → Au$_{25}$(-SCH$_2$CH$_2$Ph)$_{17}$(S-(CH$_2$)$_{11}$-OH) + HSCH$_2$CH$_2$Ph

2.

Au$_{25}$(-SCH$_2$CH$_2$Ph)$_{18}$ + HS-(CH$_2$)$_{10}$COOH → Au$_{25}$(-SCH$_2$CH$_2$Ph)$_{17}$(S-(CH$_2$)$_{10}$-COOH) + HSCH$_2$CH$_2$Ph

3.

Au$_{25}$(-SCH$_2$CH$_2$Ph)$_{17}$(S-(CH$_2$)$_{11}$-OH) + Au$_{25}$(-SCH$_2$CH$_2$Ph)$_{17}$(S-(CH$_2$)$_{10}$-COOH) $\xrightarrow{\text{DCC, DMAP}}$

Au$_{25}$(-SCH$_2$CH$_2$Ph)$_{17}$(S-(CH$_2$)$_{10}$-COO-(CH$_2$)$_{11}$-S)Au$_{25}$(-SCH$_2$CH$_2$Ph)$_{17}$

Reaction 2: Carbodiimide coupling of Au$_{25}$.

1) Alcohol functionalized Au$_{25}$ is formed by ligand exchange with 11-MUD. Amine functionalized MPC's may also be used to form amide bonds in step 3.

2) Carboxylic acid functionalized Au$_{25}$ is formed by ligand exchange of a different Au$_{25}$ sample with 11-MUA.

3) The alcohol and carboxylic acid functionalized nanoparticles are reacted with DCC and DMAP to form an ester bond linking the two MPC's. EDC and EDC-HCL have also been used as coupling reagents in place of DCC.

8

molecule. Carboxylic acid modified MPC's were then mixed with either alcohol modified or amine modified MPC's and a carbodiimide coupling reagent in methylene chloride. Catalytic amounts of 4-dimethylaminopyridine (DMAP) were added to speed ester bond formation.

There were several challenges associated with carbodiimide coupling. The carboxylic acid modified MPC's were often difficult to redisperse into organic solvents after drying. This is the result of stable attractions between individual carboxylic acid groups. The phenomenon is particularly evident with high carboxylic acid content in the monolayer, but is observed with even limited exchange. Furthermore, bond formation using this method proceeded to a much lesser degree than dithiol coupling. The extent of coupling made observation of coupled particles very difficult, and fraction collection of coupled material for analysis was not possible. The functionalized MPC starting materials used for coupling were, unlike the dithiol coupling scheme, able to be analyzed using MALDI-MS, allowing better control over the coupling reaction.

MALDI-TOF-MS Analysis of MPC's and MPC Polymers

Matrix assisted laser desorption ionization time of flight mass spectrometry (MALDI-TOF-MS) has shown recent success in resolving the molecular mass of Au_{25} clusters with single or mixed ligand monolayers.[41] For this reason, it served as an excellent starting point for the analysis of MPC dimers and substituted monomers for dimer synthesis. It was hoped that MALDI-MS would be able to observe parent ions or fragmentation patterns resulting from dimers of MPC's. While achieving this goal was

ultimately unsuccessful, MALDI-MS still proved to be an excellent tool for monitoring the extent of ligand exchange reactions for later coupling. Successful control over the polymerization process requires some knowledge of the extent of monomer substitution, and thus, the number of linkage sites that will couple the MPC's together. MALDI-MS is perfectly suited for this determination, allowing precise analysis of the extent of ligand exchange, and the polydispersity of ligand exchange products.

All MALDI-TOF-MS data was collected using an Applied Biosystems Voyager-DE Pro or Bruker Ultraflex I laser desorption linear time-of-flight mass spectrometer equipped with a nitrogen laser (337 nm). The accelerating voltage was held at 25 kV. Figure 1 shows a MALDI-MS spectrum of a 90-minute ligand exchange reaction of Au_{25} with ten incoming 4-amino thiophenol ligands per MPC core. A distribution of the number of 4-amino thiophenol ligands incorporated into the monolayer can be seen, centering on five exchanged ligands, and ranging from three to seven exchanged ligands.

Figure 2 shows an example of determining ligand exchange products from a ligand exchange with 11-amino-1-undecanethiol. In this example, no parent ion peaks are observed, so the fragmentation pattern of the MALDI spectrum is used to show the extent of exchange. The arrows in the figure point out fragmentation peaks showing an 11-amino-1-undecane thiol substituted fragment, and a corresponding fragment that consists of only phenylethanethiol ligands. While the extent of ligand exchange has not been quantified, 11-amino-1-undecanethiol incorporation into the monolayer has been shown. However, the lack of a fragment peak showing two 11-amino-1-undecanethiol ligands suggests that the likely extent of ligand incorporation is either zero or one incoming ligand per MPC core.
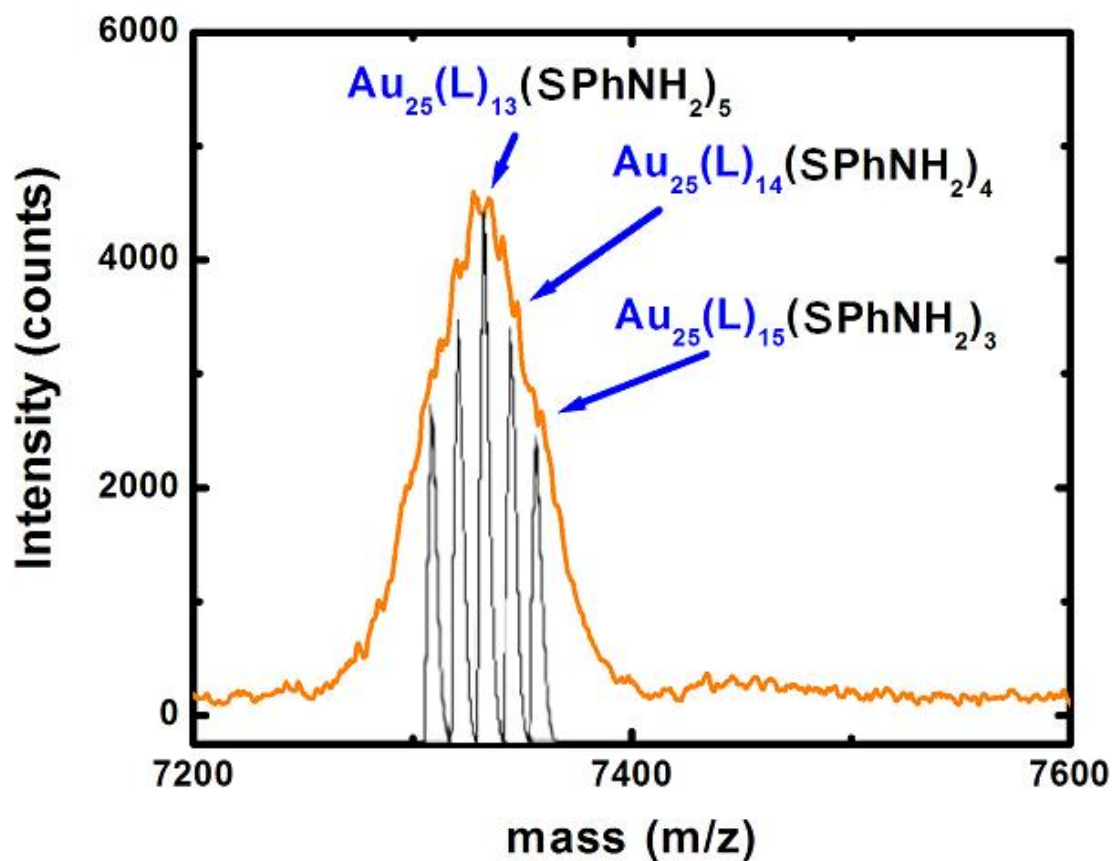
10

Figure 1: MALDI-TOF-MS spectrum of $Au_{25}(SCH_2CH_2Ph)_{18-x}(SPhNH_2)_x$ where x is the number of exchanged ligands. Au_{25} was mixed with 4-amino thiophenol in a ratio of ten incoming ligands per MPC core with stirring for 90 minutes. A distribution of ligand exchange is observed, centering on five exchanged ligands, and ranging from three to seven exchanged ligands. The orange trace shows the experimental MALDI data, while the black trace represents the theoretical spectrum for $Au_{25}(SCH_2CH_2Ph)_{11-15}(SPhNH_2)_{3-7}$.
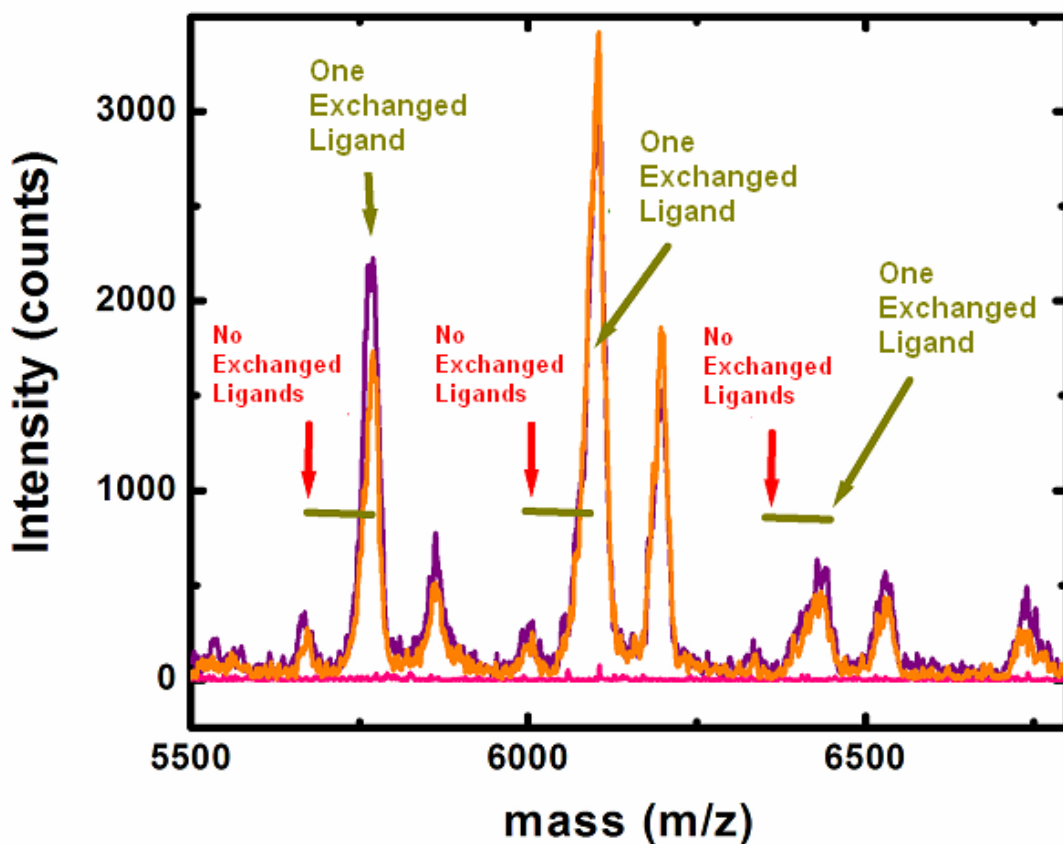
Figure 2: MALDI-TOF-MS spectrum of $Au_{25}(SCH_2CH_2Ph)_{18-x}(S(CH_2)_{11}NH_2)_x$ fragmentation, where x is the number of exchanged ligands ranging zero to one. Au_{25} was mixed with 11-amino-1-undecanethiol in a ratio of ten incoming ligands per MPC core with stirring for 30 minutes (purple trace) or 90 minutes (orange trace). Arrows point to pairs of peaks representing the same fragment species possessing either zero (red arrows) or one (green arrows) exchanged 11-amino-1-undecanethiol ligand. Horizontal lines connect the unsubstituted Au_{25} peak with a peak of the same fragment ion having one 11-amino-1-undecanethiol substitution. In this way, the fragmentation pattern indicates presence of 11-amino-1-undecanethiol substituted into the monolayer.

MALDI-MS has been thus far unsuccessful, however, in observing coupled MPC's. Figure 3 shows MALDI-MS spectra obtained from Au_{25} as well as an ester bond coupling reaction between 11-mercaptoundecanoic acid (11-MUA) and 11-mercaptoundecanol (11-MUD) substituted Au_{25} MPC's. No peak can be seen for a single charged dimer peak. The inset of Figure 3 shows an expansion of the Au_{25} parent ion region of the coupling product spectra. Ligand exchange products can be seen for monosubstituted 11-MUA as well as mono- and disubstituted 11-MUD particles. The presence of any doubly charged MPC dimer species is lost among these singly charged substituted MPC monomer peaks. Similar reactions of 11-MUA substituted MPC's with small molecule alcohol, amine, or diol linking agents failed to produce a recognizable Au_{25} parent ion peak, and the fragmentation patterns were of too low an intensity to allow further analysis, as shown in Figure 4. While unable to observe MPC coupling products, MALDI data was useful in preparing batches of MPC with a small extent of coupling site exchange for analysis by liquid chromatography.
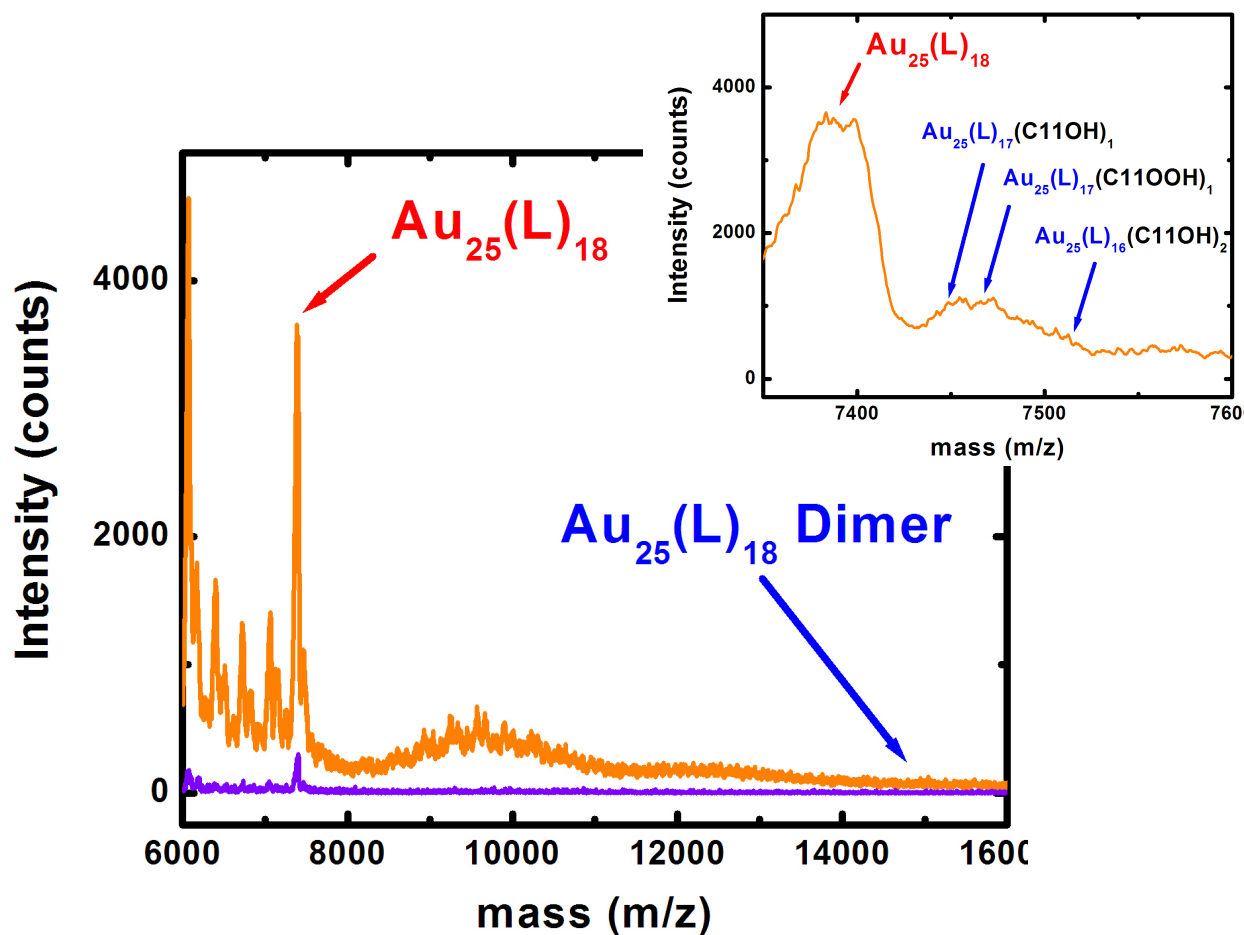
Figure 3: MALDI-TOF-MS of Au_{25} and an ester coupling reaction. 11-MUA and 11-MUD substituted MPC's (1mg each) were combined with 1 equivalent of DCC and catalytic DMAP in DCM with stirring in the dark overnight. MALDI-TOF-MS analysis of the resulting product is shown in the purple trace, while the orange trace shows unsubstituted Au_{25} starting material. The Au_{25} dimer peak is not present in either spectrum.

Inset: The Au_{25} parent ion peak from the coupling reaction above. MUA and MUD substituted Au_{25} overlaps the location of a possible doubly charged Au_{25} dimer.
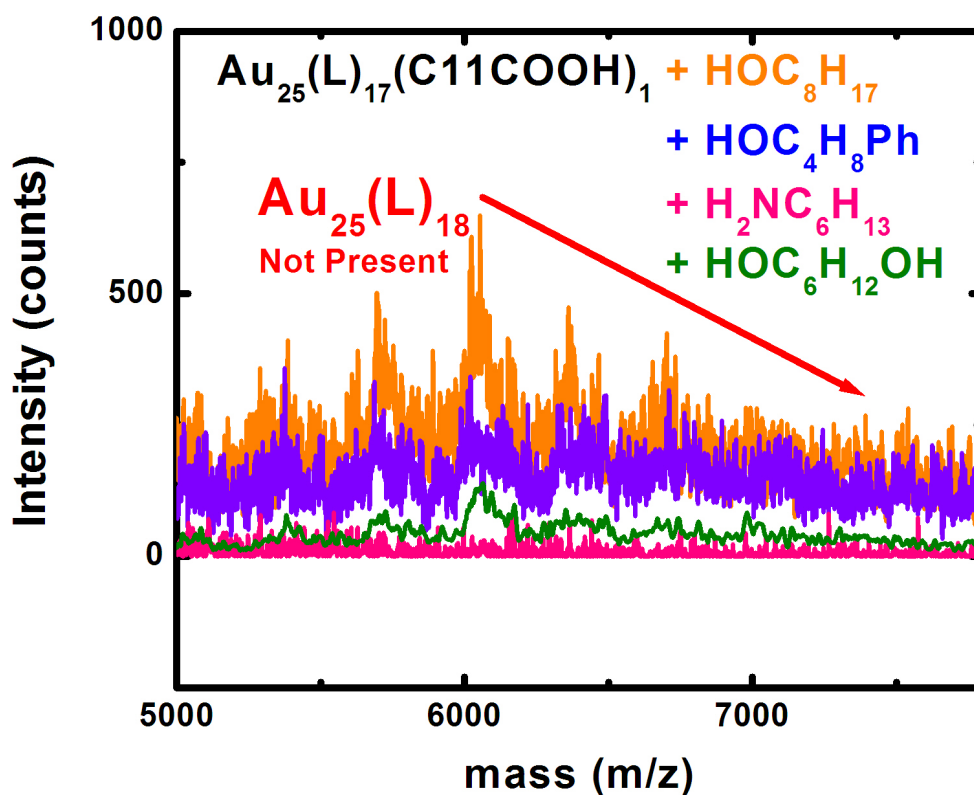
Figure 4: MALDI-TOF-MS showing various coupling products. 11-MUA substituted Au₂₅ was reacted with 1 equivalent of DCC and either 1-octanol (orange), 1-phenyl-4-butanol (blue), 1-amino hexane (pink), or hexane diol (green). No Au₂₅ parent ion is present, and fragmentation is of greatly decreased intensity relative to unsubstituted Au₂₅.

Separation of MPC Polymers

Size Exclusion Chromatography of MPC Polymers:

High performance size exclusion liquid chromatography (SEC) was used to separate

reaction mixtures of dithiol linked MPC's. The experiments were carried out using a

Waters 600 controller pump with a Waters 996 PDA detection system. All

chromatograms shown are presented at 400nm. Injections were made using a Rheodyne

7725 injection valve with a 50μL loop. Two Thermo Scientific Hypergel OP10

polystyrene/divinylbenzene SEC columns (100Å pore size) were used in series for

separation. Optimum pore size was obtained by determining the ratio of inner volume of

the pore that the particle can exist within the outer volume of the entire pore (see Figure

5). Optimal separation is achieved at a ratio of one half, at which point the monomer will

be retained by half the total retention ability of the column. A 100Å pore size column

gives a ratio of inner volume to outer volume of 0.64 based on the monomer MPC

diameter of Au_{25} of 22 angstroms.

   Purified Au_{25} gives a single retention peak using these columns, as shown in

Figure 6, with a small amount of slightly larger material eluting just before the peak. The

main peak shows the characteristic step-like absorbance features of Au_{25}, while the

material eluting before the peak has a more featureless absorbance spectra indicative of

larger nanoparticles.

   The Au_{25} starting material was then coupled using octane dithiol linkers (10

linkers per MPC core) in dichloromethane with stirring overnight. The reaction mixture

was filtered with a 45μm syringe filter. The result is a shift in the position of the main
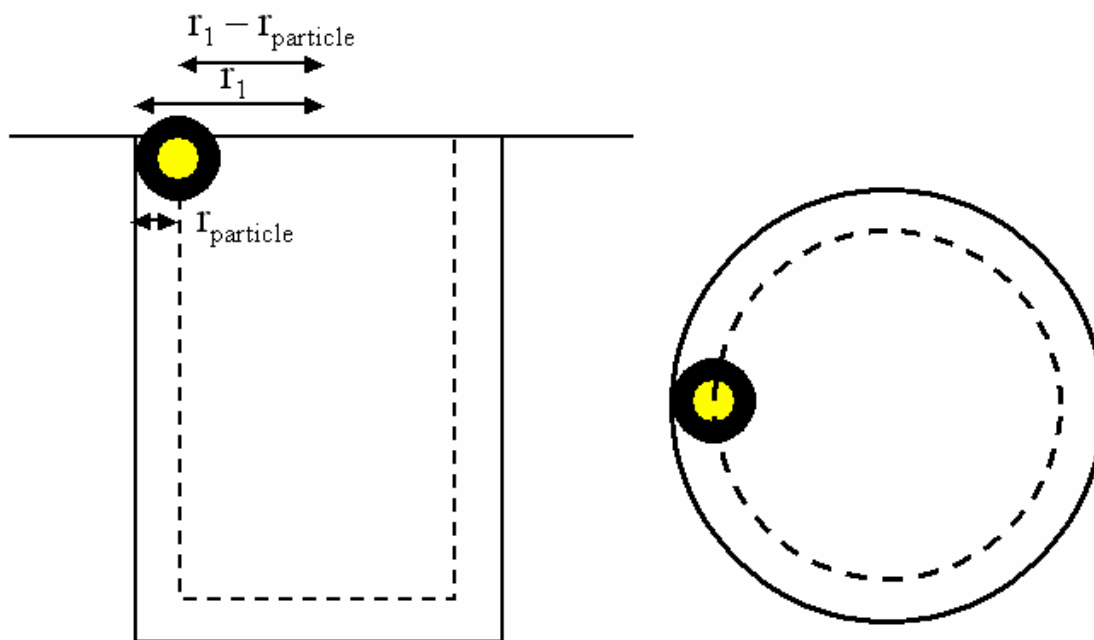
Figure 5: Cartoon representation of a gold MPC in an ideal SEC pore. The inner volume is determined by the volume in which the center of the particle can exist (r_1-$r_{particle}$) while the outer volume is given by the entire volume of the pore. Optimal pore size can be determined by setting the ratio of inner to outer volume equal to one half. The 100Å pore size columns used give a inner to outer volume ratio of 0.64 based on the monomer MPC diameter of Au_{25} of 22 angstroms.
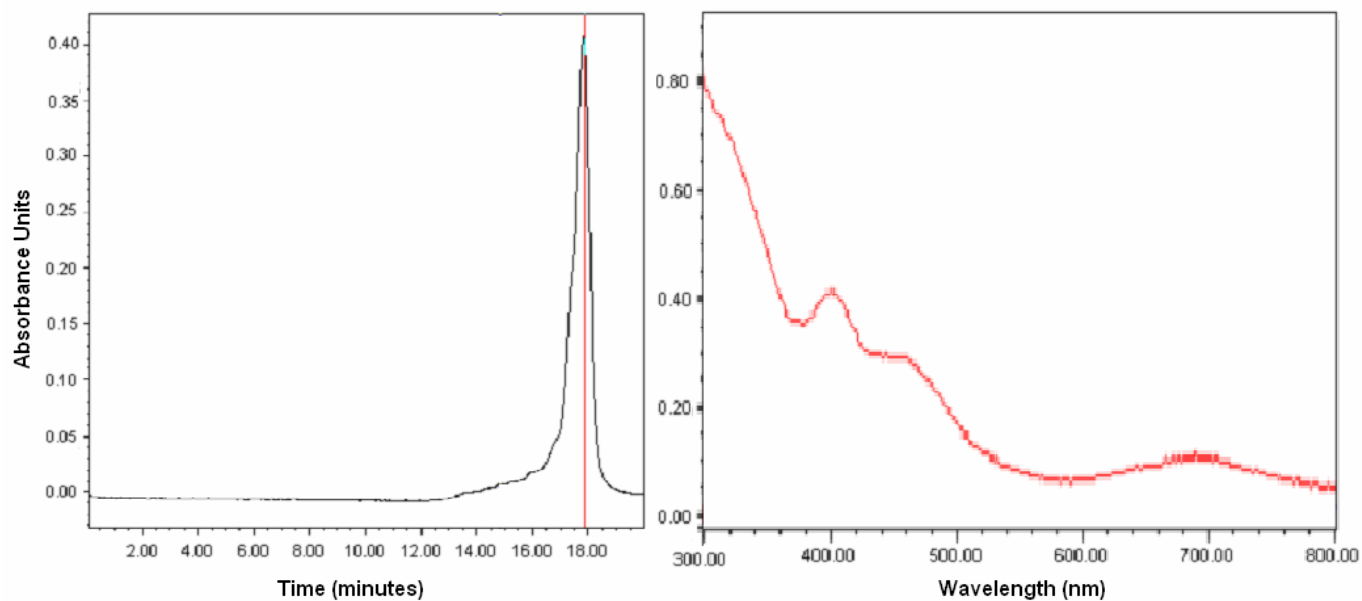
Figure 6: SEC chromatogram of Au$_{25}$ separated on two Thermo Scientific Hypergel OP10 polystyrene/divinylbenzene SEC columns (100Å pore size) in a DCM mobile phase flowing at 0.7mL/min. The main peak shows the characteristic Au$_{25}$ step-like UV-visible absorbance spectra. A small amount of larger particles, with smoothed out UV-visible absorbance spectra, elute just before the main peak.

peak to a lower retention time and an increase in the absorbance of the smaller peaks

before the main peak, as seen in Figure 7a. This suggests larger MPC molecules.

Doping the sample with unreacted Au_{25}, Figure 7b, proves that the retention time

difference is a result of a change in the analyte and not the SEC system. The UV-visible

absorbance remains unchanged in the coupled product, indicating that a core size change

was unlikely the cause of the shift in retention.

A biphenyl dithiol linker was also used to bridge MPC's. The stiff biphenyl

molecule prevents twisting of the linker from slowing down the coupling reaction, as was

possible with an octane dithiol linker. The biphenyl dithiol molecule is also structurally

similar to thiophenol, which as been shown to have very fast ligand exchange kinetics.

This increases the likelihood of formation of the MPC polymer. Finally, the biphenyl

dithiol linker was chosen for its conjugated structure, which allows electronic connection

between linked MPC cores that was not possible with the insulating octane dithiol

molecule. Figure 8 shows the chromatogram and UV-visible absorption spectra at

several retention times. The UV-visible spectra of the lower retention time peaks

changes dramatically relative to unreacted Au_{25}, losing the characteristic step-like

structure associated with the Au_{25} monomer while a new absorbance band grows in at

330nm. This change was not observed even in comparable retention times resulting from

the coupling of MPC's using octane dithiol, which showed characteristic Au_{25} UV-visible

absorbance. The absorbance spectrum of the main peak from the biphenyl dithiol

coupling remains unchanged. The change in the spectrum of biphenyl dithiol coupling is

believed to result from the electronic interactions between linked MPC's through the

conjugated linker. The octane dithiol bridge acts as an insulator, preventing electronic
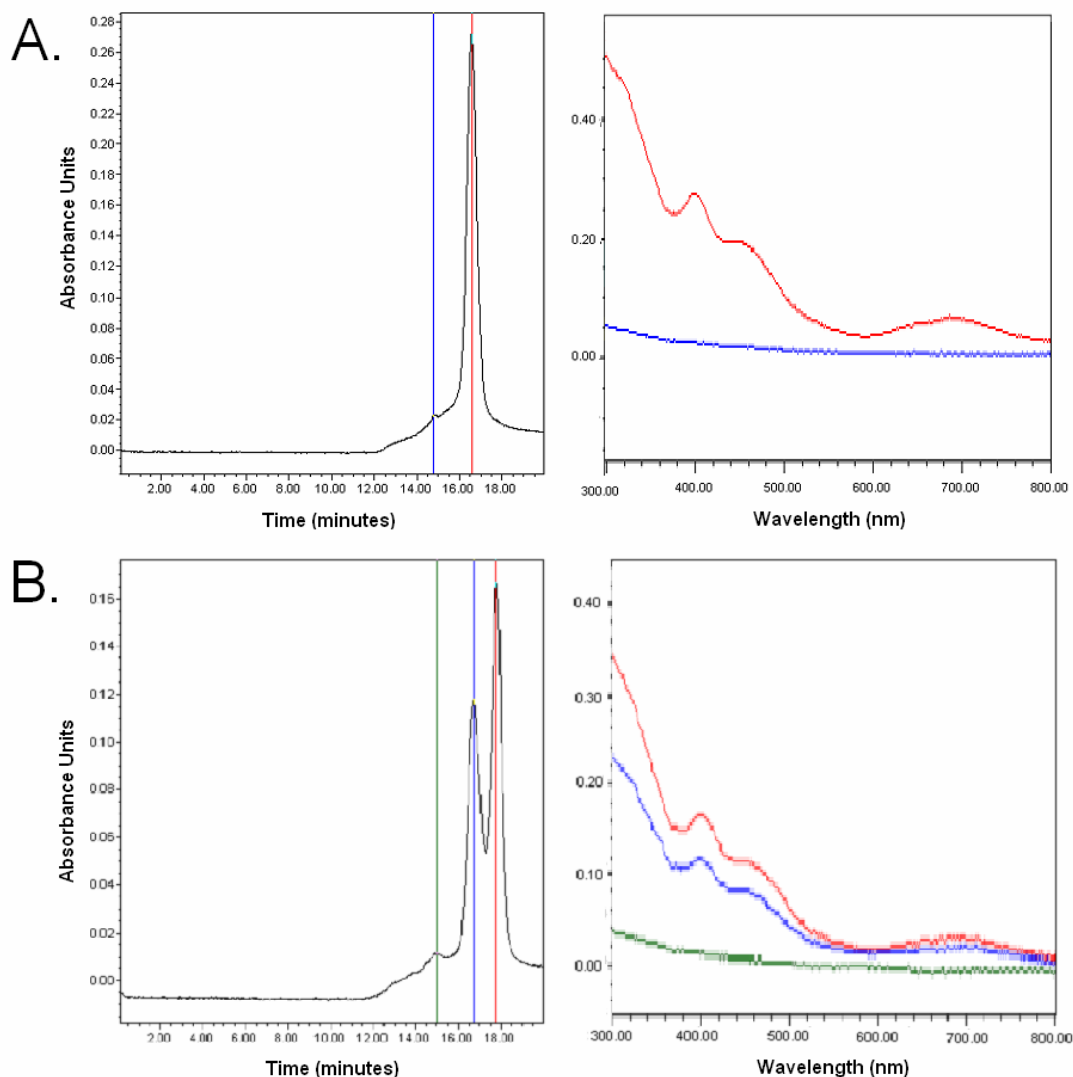
Figure 7: a) An SEC chromatogram of octane dithiol coupled Au_{25} separated on two Thermo Scientific Hypergel OP10 polystyrene/divinylbenzene SEC columns (100Å pore size) in a DCM mobile phase flowing at 0.7mL/min. Au_{25} was mixed with octane dithiol (10 linkers per MPC core) in DCM with stirring overnight, and filtered with a 45μm syringe filter. The resulting SEC chromatogram appears similar to that of the Au_{25} starting material. The main peak exhibits a typical Au_{25} UV-visible absorbance spectrum.

b) The above sample was mixed with unreacted Au_{25} and separated using SEC. The difference in retention time between the coupled reaction product and the unreacted starting material can be clearly seen.
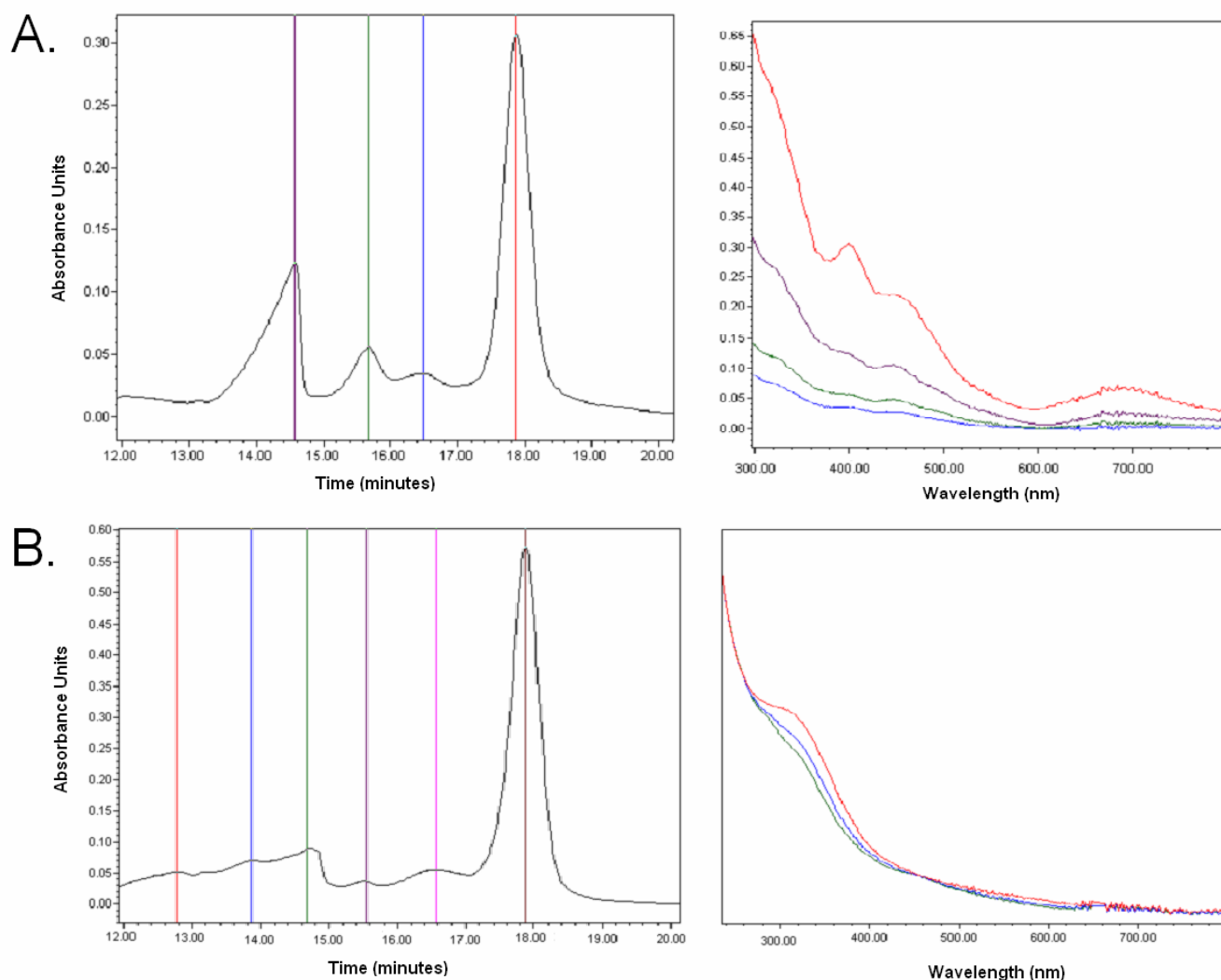
Figure 8: a) SEC chromatogram of octane dithiol coupled MPC's separated on two Thermo Scientific Hypergel OP10 polystyrene/divinylbenzene SEC columns (100Å pore size) in a DCM mobile phase flowing at 0.7mL/min. MPC's were mixed with octane dithiol (one linker per two MPC cores) for 5 ½ hours with stirring in DCM. The UV-visible absorbance spectra show characteristic step-like structure for each eluting peak. b) Chromatogram of biphenyl dithiol coupled MPC's under the same chromatographic conditions. MPC's were mixed with biphenyl dithiol (one linker per two MPC cores) for 12 hours with stirring in DCM. The main peak and later eluting peaks show step-like structure indicative of Au_{25}, while the earliest eluting peaks show marked difference in the UV-visible spectra as shown, losing the step-like structure while a new absorbance band grows in at 330nm.

interactions between coupled particles. Thus, the absorbance spectra for these coupling products appears as that of the uncoupled monomers.

Aliquots of the dithiol coupling reaction mixture were also analyzed over time to understand how the coupling reaction proceeds. Figure 9a shows chromatograms taken from aliquots of a reaction of approximately two MPC cores for each octane dithiol linker in dichloromethane. At much longer reaction times, insoluble material was observed, leading to the belief that the actual dithiol content was higher than expected and resulting in larger MPC polymers. The main peak, MPC monomer, remains unchanged throughout. Longer reaction times appear to show the formation of three unique populations of linked MPC's, shifting slowly towards shorter retention times while remaining constant in relative peak height. The large amount of fronting present in the earliest eluting peak is indicative of decreased solubility in the mobile phase.

An interesting phenomenon is observed, however, when the samples are rotary evaporated to dryness and redispersed in dichloromethane. This was done for samples taken at 8 hours and 24 hours, and resulted in a large amount of insoluble material. It is believed that the high concentration of MPC in a very small volume during rotary evaporation led to the increased formation of dithiol linkages from previously monosubstituted MPC-dithiols. That is, some of the populations present in Figure 9a before rotary evaporation could be an MPC monomer attached to one end of a dithiol molecule, with the other thiol end still free. During the removal of solvent, the free thiol end becomes bound to a new MPC. The result is dramatically shown in Figure 9b-c, showing chromatograms of the 8- and 24-hour reaction time aliquots after rotary evaporation, filtering using a 45μm syringe filter, and separation by SEC. The increased
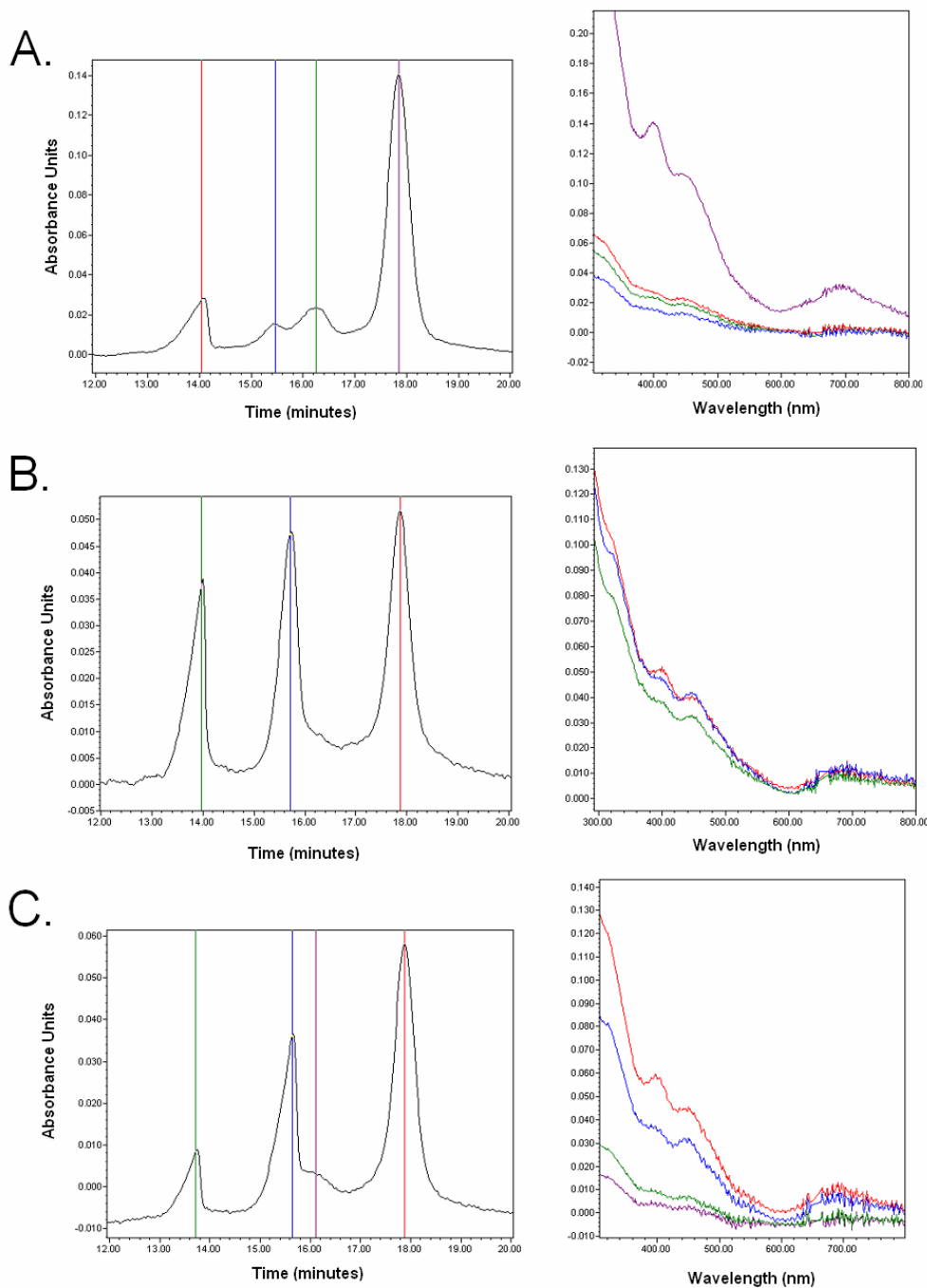
Figure 9: a) SEC chromatogram of octane dithiol coupled MPC's separated on two Thermo Scientific Hypergel OP10 polystyrene/divinylbenzene SEC columns (100Å pore size) in a DCM mobile phase flowing at 0.7mL/min. MPC's were mixed with octane dithiol (one linker per two MPC cores) for 24 hours with stirring in DCM, and filtered with a 45μm syringe filter before separation by SEC. The UV-visible absorbance spectra show characteristic step-like structure for each eluting peak.

b) An aliquot was taken from the sample in (a) above after 8 hours of reaction time, and rotary evaporated to dryness. The sample was then redissolved in DCM, filtered with a 45μm syringe filter before separation by SEC under the same chromatographic conditions.

c) The same procedure from (b) above was followed with an aliquot taken from (a) after 24 hours reaction time.

fronting in the less retained species again suggests decreased solubility in the mobile phase.

Reversed Phase Chromatography of MPC Polymers:

Reversed phase high performance liquid chromatography, utilizing the same experimental system as described above, was used to analyze the carbodiimide coupled nanoparticles. Thermo Scientific Hypersil BDS (120Å pore size, 250 x 4.6mm i.d. stainless steel, silica bonded C18 or phenyl) or Thermo Scientific Biobasic (300Å pore size, 250 x 4.6mm i.d. stainless steel, silica bonded C4 or C8) columns were used in place of the SEC columns. Both 140 gold atom and 25 gold atom clusters were analyzed using this system.

Chromatography of Au_{140} shows much greater polydispersity than Au_{25}. This is evident in multiple, broad peaks when separated by RP-HPLC. Using an annealing process as described above increases sample monodispersity. RP-HPLC was first used to try to resolve ligand exchange reactions onto Au_{140}. Figure 10 shows chromatography of annealed Au_{140} and Au_{140} after exchange with mercapto-1-hexanol (one hundred incoming ligands per MPC core) for 34 hours. While ligand exchange can be seen to have an effect on the retention time in this case, no resolution of exchange products can be seen. Furthermore, the affect of ligand exchange can only be observed using RP-HPLC when the particles have undergone a large amount of ligand exchange. Only a few ligands incorporated into the monolayer, which would be required for coupling reactions to prevent large polymerization products, fails to provide an observable difference in partition.
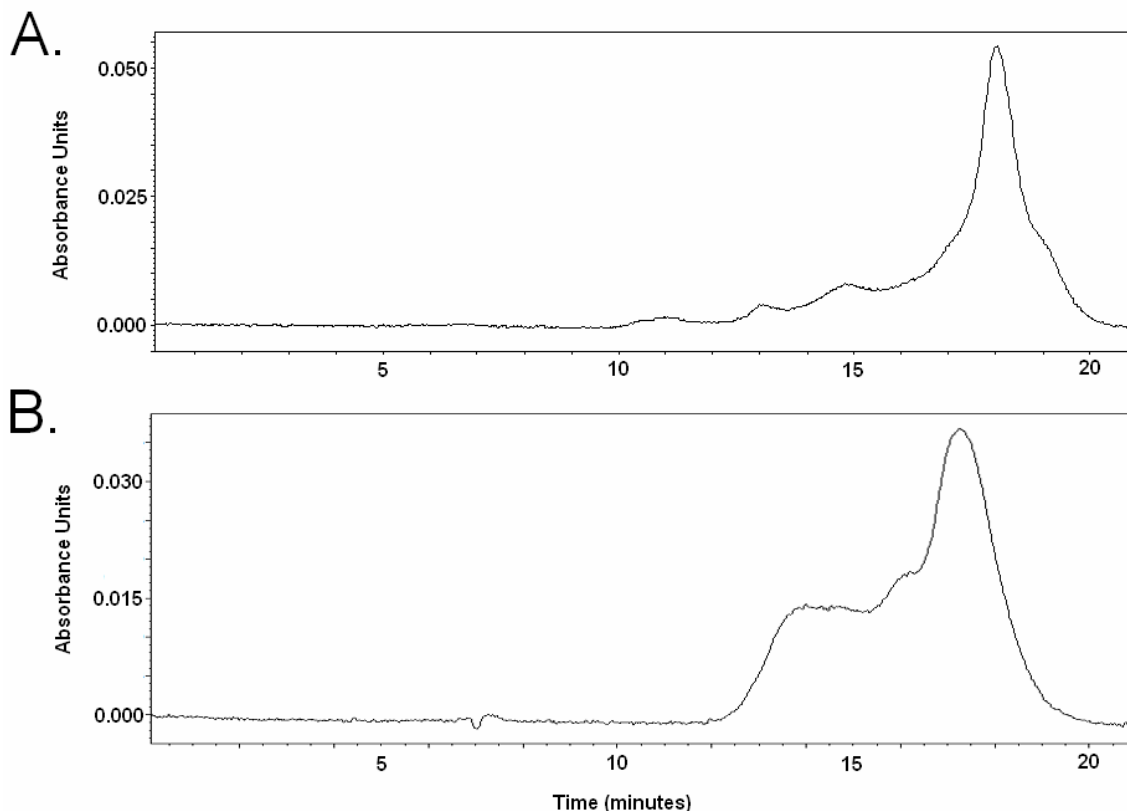
Figure 10: a) A reverse phase HPLC chromatogram of annealed $Au_{140}(SC_6H_{12})_{53}$ separated on aThermo Scientific Hypersil BDS C18 column and a Thermo Scientific Hypersil BDS phenyl column in series using a DCM mobile phase at 0.7mL/min.. Au_{140} was annealed in DCM with the addition of 100 hexane thiol ligands per core ligand in the dark overnight to increase monodispersity of the sample.

b) The above sample then underwent ligand exchange with 100 mercapto-1-hexanol ligands per MPC core (5.6 incoming ligands per core ligand) in DCM for 34 hours, and the chromatogram shown here was obtained using the same chromatographic conditions. Mercapto-1-hexanol incorporated into the protecting monolayer increased the polarity of exchanged particles, resulting in less interaction with the stationary phase, and a shorter retention time. Incomplete resolution of peaks was seen, however.

Au$_{25}$ has also been separated using RP-HPLC for the purpose of detecting ligand exchange and observation of coupled particles. Synthesis of Au$_{25}$ without purification by several extractions into acetonitrile has been shown to obscure the characteristic UV-visible absorbance spectra, as shown in Figure 11a-b, while eluting as a single broad peak or several poorly resolved peaks. Numerous extractions into acetonitrile results in a single defined peak for the Au$_{25}$ species, as shown in Figure 11c. Limited ligand exchange reactions, however, still do not produce an adequate difference in partitioning to allow resolution of exchanged MPC's.

RP-HPLC has shown limited success in separating coupled MPC products. Au$_{25}$ substituted with 11-MUA ligands were coupled to hexane thiol using DCC, and the resulting mixture was analyzed as shown in the chromatogram in Figure 12. The increase in non-polar character relative to the carboxylic acid chains is believed to be responsible for the peaks at higher retention time. Figure 13 shows chromatograms taken from the methanol soluble and insoluble fractions of DCC coupled 11-MUA and 11-MUD substituted MPC's. Here again, the higher retention time peaks are believed to result from the increased non-polar character of the coupled nanoparticles. To further extrapolate from this trend, experiments were carried out to couple a very non-polar molecule, cholesterol, to 11-MUA functionalized MPC's. This coupling reaction, however, resulted in a great deal of insoluble material, and the soluble material proved difficult to elute from the reversed phase columns.
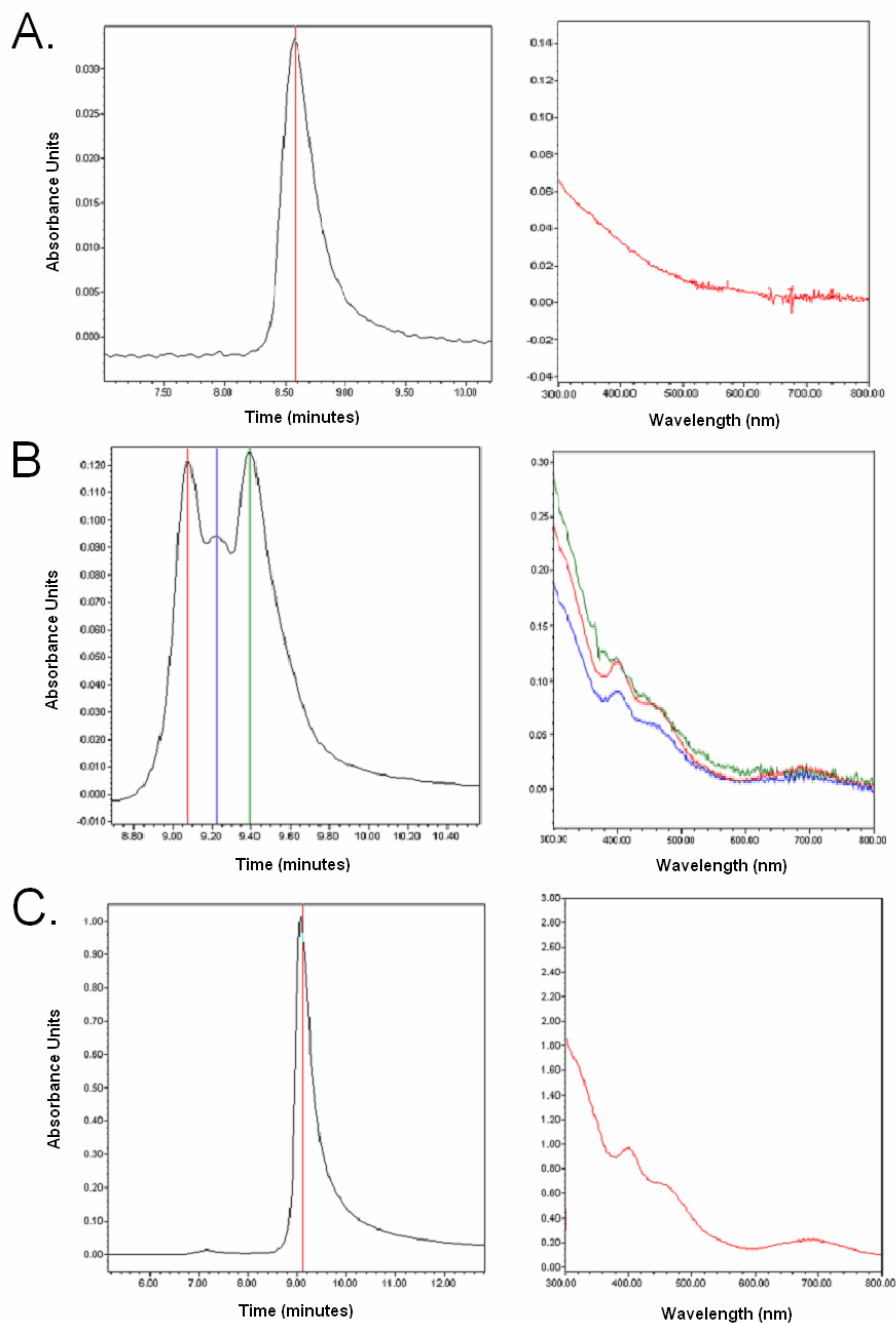
Figure 11: a) Au$_{25}$ prepared as described previously before extraction into acetonitrile, separated on a Thermo Scientific Biobasic C8 and Thermo Scientific Biobasic C4 column in series with a DCM mobile phase at 0.7mL/min. One broad peak is observed, with no characteristic Au$_{25}$ spectral features.

b) The same particles from (a), extracted into acetonitrile with some stirring, and separated under the same chromatographic conditions. Three poorly resolved peaks are observed, showing step-like Au$_{25}$ spectral features.

c) The same particles from (a), extracted twice into acetonitrile with no stirring, and separated under the same chromatographic conditions. A single peak is obtained, clearly showing the characteristic step-like Au$_{25}$ spectral features.
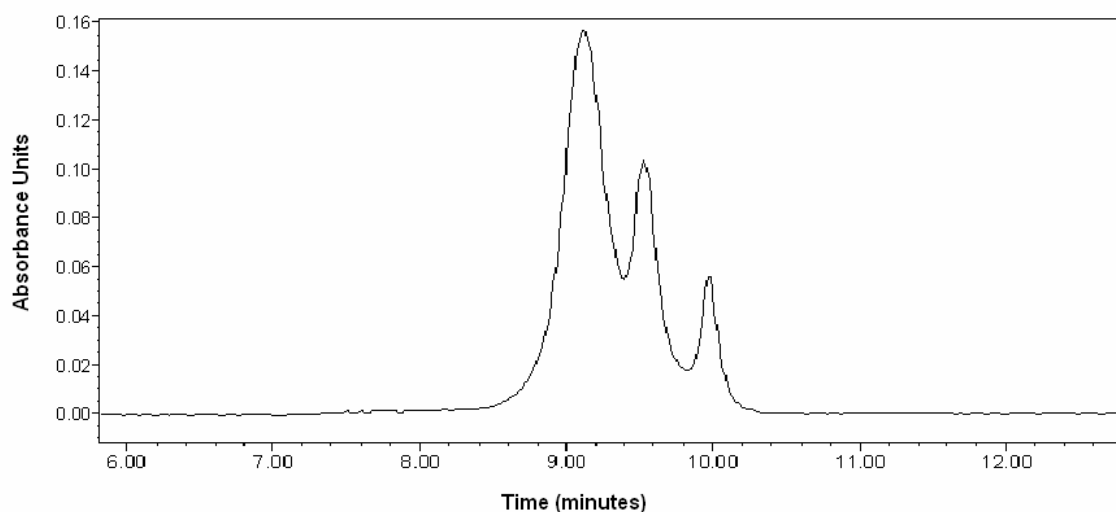
28

Figure 12: Au$_{25}$ was substituted with 11-MUA prepared as described previously, and separated on a Thermo Scientific Biobasic C8 and Thermo Scientific Biobasic C4 column in series with a DCM mobile phase at 0.7mL/min. The particles were then DCC coupled to 1-hexanol in DCM. The higher retention time peaks are believed to result from the decrease in polar character of the hexane terminated ligands of the coupled particles relative to the free carboxylic acid ligand termination prior to coupling.
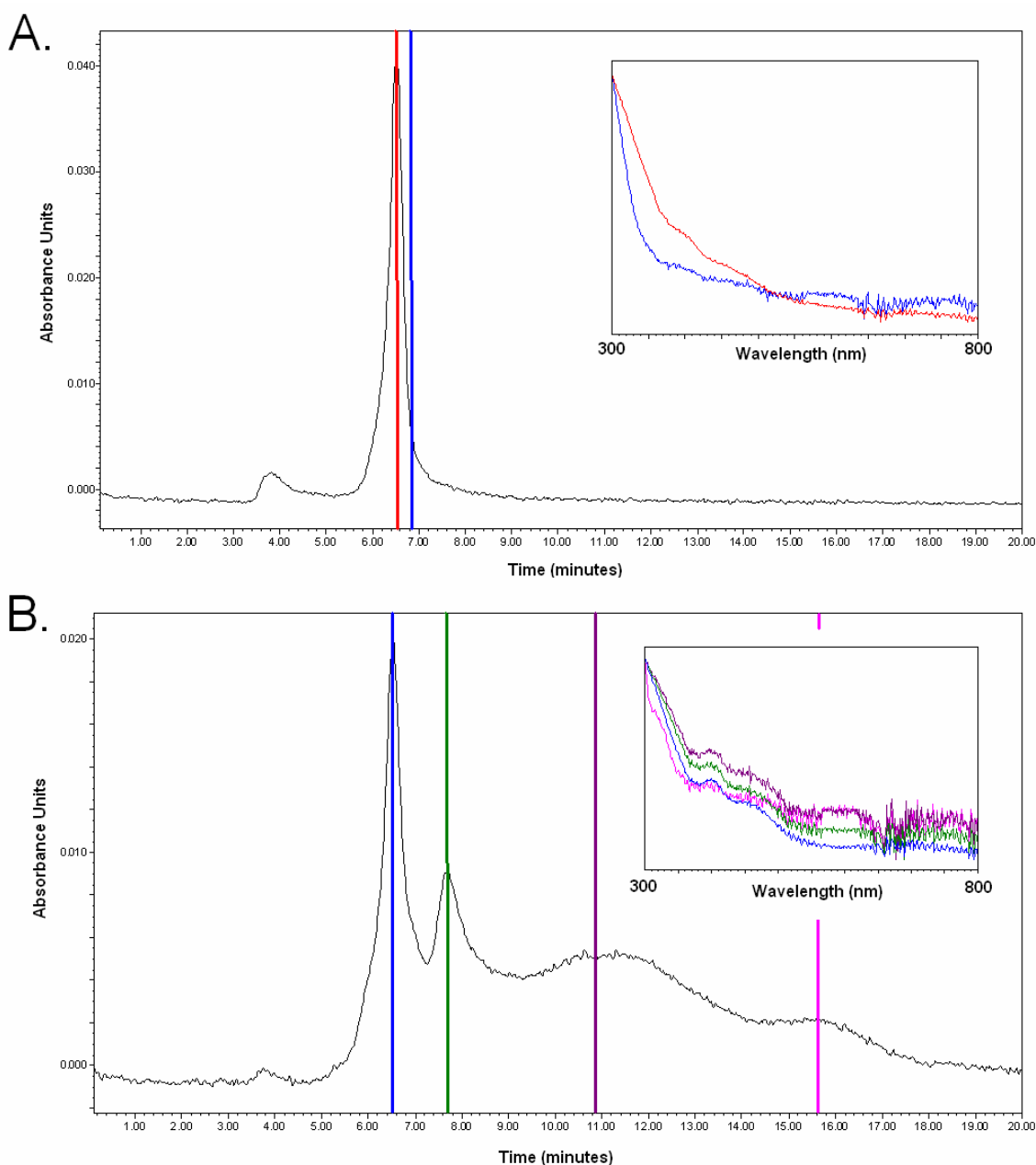
Error!

Figure 13: Two populations of Au_{25} MPC's were prepared, one having undergone ligand exchange with 11-MUD and the other with 11-MUA. They were then mixed together with 1 equivalent of DCC in DCM to couple the particles via an ester bond. The resulting particles were washed with methanol, and the methanol soluble portion was separated as shown in chromatogram (b). The large retention time peaks, showing the step-like absorbance features of Au_{25}, are believed to be the coupled MPC's. The remaining particles after the methanol rinse were dissolved in DCM, and are shown in separated in chromatogram (a). Separations were carried out on a Thermo Scientific Biobasic C8 and Thermo Scientific Biobasic C4 column in series with a DCM mobile phase at 0.7mL/min.

Analysis of Collected SEC Fractions

Fraction collection of the SEC separated coupling products was also used to further analyze the larger species. Typically, the peak intensities for the larger products were too low to allow for individual analysis, so combination of the low retention time peaks from several runs was necessary. Fractions analyzed by MALDI-MS revealed an increase in the relative amount of high mass fragments for earlier eluting fragments, as shown in Figure 14, although no parent ion peak was observed. Fractions collected from the main peak in the chromatogram showed typical voltammetry for Au_{25} using a 1 mm platinum working electrode, platinum counter electrode, and silver quasi-reference electrode at 100mV/sec. No voltammetric response was seen for the smaller peaks, even at decreased scan rates. The lack of signal is, however, believed to be a function of MPC concentration.

High mass fragments were also analyzed by transmission electron microscopy (TEM), as seen in Figure 15. The images show a highly polydisperse mixture, composed of clumps of particles. Figure 15b shows a section of the larger TEM image, with lines measuring 1.0 to 1.2nm over various parts of the clumps of MPC's. They suggest that each clump of MPC's is, in fact, composed of several 1.1nm particles in direct proximity. Analyzing the distance between cores reveals several distinct populations of MPC spacing. The first population are those in direct proximity to another particle. The other three populations, shown in the histogram in Figure 16, are ~1.1 nm (two phenylethanthiol ligands end to end, or one octane dithiol bridge), ~1.6nm (one phenylethanethiol and one monosubstituted octane dithiol ligand end to end), and ~2.1nm (two monosubstituted octane dithiol ligands end to end). The 2.1 nm spacing may also be

the result of a disulfide formation between two monosubstituted octane dithiol ligands. These images lend strong credibility to the presumed linkages observed by SEC separation, but it is important to note that some coupling may also have resulted post-column while the sample was being concentrated for application on the TEM grid.
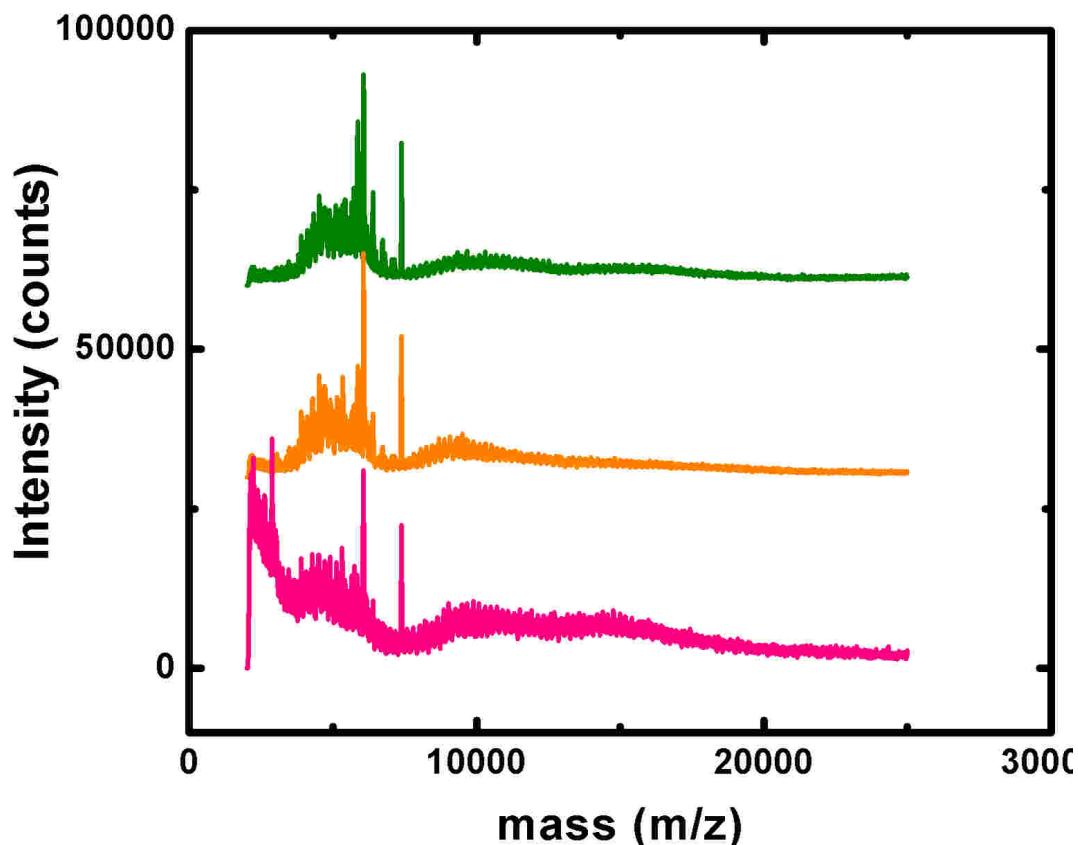

Figure 14: MALDI-TOF-MS spectra of fraction collected Au_{25} samples, normalized to the Au_{25} parent molecular ion peak at 7400. The green trace shows the dithiol coupled MPC's (one dithiol linker per two MPC cores in DCM for 12 hours) before separation. The particles were then separated on two Thermo Scientific Hypergel OP10 polystyrene/divinylbenzene SEC columns in a DCM mobile phase flowing at 0.7mL/min, and fractions were collected for MALDI-TOF-MS analysis from the main peak (orange trace) and a combination of all fractions eluting before the main peak (pink trace). Notice the concentration of high mass fragments (10-20 kDa) in the pink trace, believed to be the result of dithiol linked MPC's.
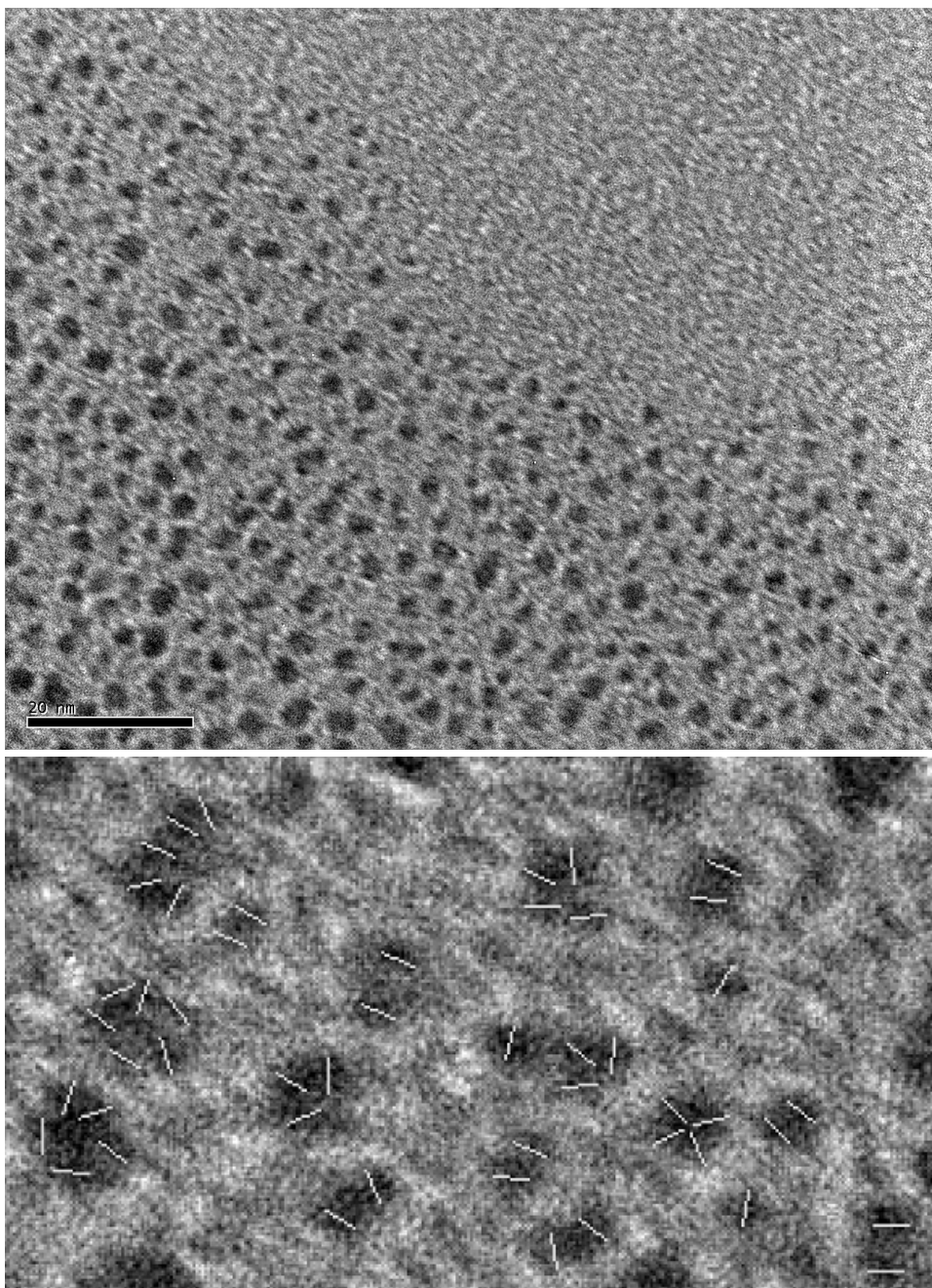
Figure 15: a) The combined fractions from the pink curve in Figure 14, comprised of several combined peaks eluting before the main MPC peak on two Thermo Scientific Hypergel OP10 polystyrene/divinylbenzene SEC columns , were analyzed using TEM. Clumps of nanoparticles can be seen in this image. The scale bar measures 20nm, and the clumps of MPC's measure between 1 and 3 nm.

b) An enlargement of the image reveals clumps of MPC's composed of smaller 1.1nm particles, corresponding to the core size expected for Au_{25}. The white scale lines drawn over the MPC clumps denote smaller particles, and each measure between 1.0 and 1.2nm.
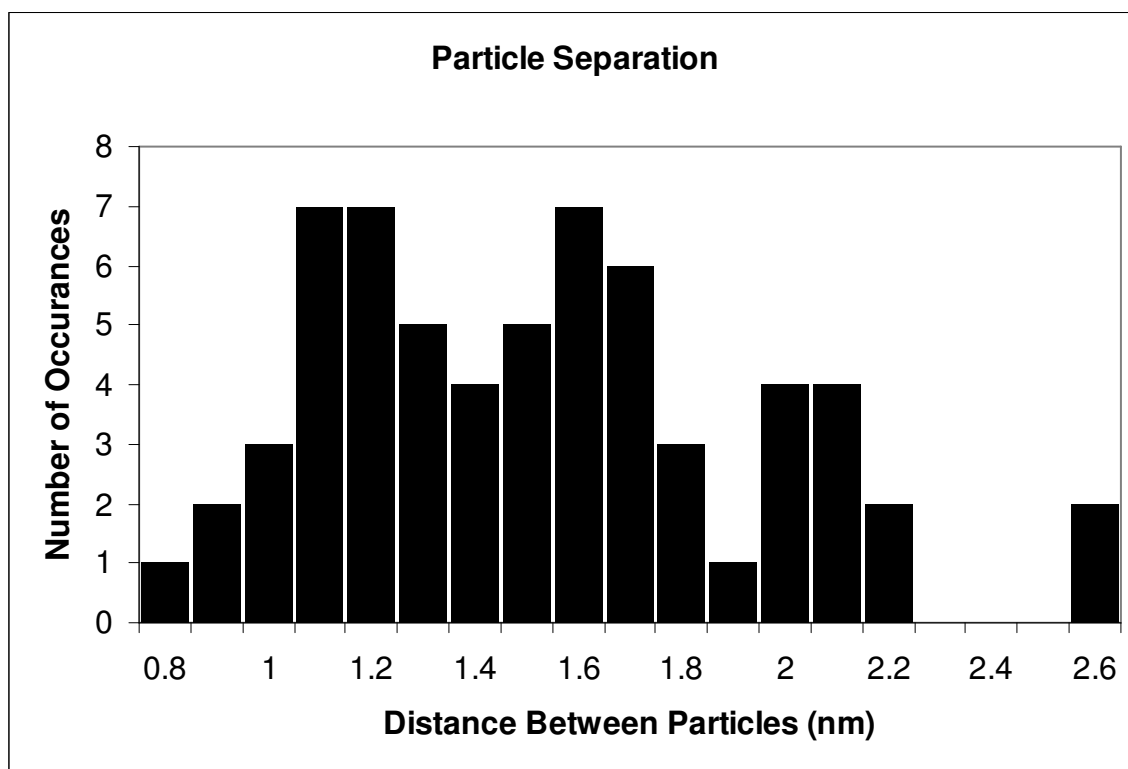
Particle Separation

Figure 16: A histogram of the separation between particles observed via TEM as shown in Figure 15(a). Besides directly adjacent (zero spacing) distances between particles, three populations of inter-particle separation can be seen. They correspond to two phenylethanthiol ligands end to end or one octane dithiol bridge (~1.1nm), one phenylethanethiol and one monosubstituted octane dithiol ligand end to end (~1.6nm), and two phenylethanethiol ligands end to end (~2.1nm).

Conclusion

This report has detailed the progress made in the synthesis, separation, and characterization of small-chain MPC polymers. However, further work is required to allow these materials to be used in the study of electron transfer dynamics between linked cores.   Refinement of the synthetic and chromatographic methods must progress from analytical methods to preparative techniques to allow sufficient materials to be collected for further study. With increased specificity of MPC polymer size and linkers, as well as increased yield from preparation and separation of these materials, electrochemical studies will be possible, by which electronic interactions can be more thoroughly explored.

Much has been accomplished to make these studies possible. MALDI-MS has been used to classify mixed monolayer starting materials, as well as to search for direct evidence of MPC polymers. Dithiol linkers and carbodiimide ester or amide formation have shown evidence of linked MPC polymers. HPLC and SEC have been used to separate complex mixtures of reaction products and isolate MPC polymers, which have then been collected and analyzed using TEM and MALDI-MS. This report hopes to have laid the groundwork for future research into the electonics of gold MPC's through the use of small-chain MPC polymers.

References

(1) Liu, J.; Lu, Y. *J.; Am. Chem. Soc.* **2003**; *125*; 6642.

(2) Perez, J. M.; Simeone, F. J.; Saeki, Y.; Josephson, L.; Weissleider, R. *J.; Am. Chem. Soc.* 125; 10192.

(3) Adams, D. M.; Brus, L.; Chidsey, C. E. D.; Creager, S.; Creutz, C.; Kagan, C. R.; Kamat, P. V.; Lieberman, M.; Lindsay, S.; Marcus, R. A.; Metzger, R. M.; Michel-Beyerle, M. E.; Miller, J. R.; Newton, M. D.; Rolison, D. R.; Sankey, O.; Schanze, K. S.; Yardley, J.; Zhu, X; *J. Phys. Chem. B* **2003**; *107*; 6668.

(4) Brennan, J. L.; Branham, M. R.; Hicks, J. F.; Osisek, A. J.; Donkers, R. L.; Georganopoulou, D. G.; Murray, R. W.; *Anal. Chem.* **2004**; 76; 5611.

(5) Lee, D.; Donkers, R. L.; DeSimone, J. M.; Murray, R. W.; *J. Am. Chem. Soc.* **2003**; 125, 1182.

(6) Donkers, R. L.; Lee, D.; Murray, R. W.; *Langmuir* **2004**; 20; 1945.

(7) Hicks, J. F.; Templeton, A. C.; Chen, S.; Sheran, K. M.; Jasti, R.; Murray, R. W.; Debord, J.; Schaff, T. G.; Whetten, R. L.; *Anal. Chem.* **1999**; 71; 3703

(8) Ingram, R. S.; Hostetler, M.J.; Murray, R. W.; Schaff, T. G.; Khoury, J. T.; Whetten, R. L.; Bigioni, T. P.; Gurthrie, D. K.; First, P. N. *J. Am. Chem. Soc.* **1997**; 119; 9279.

(9) Chen, S.; Ingram, R. S.; Hostetler, M. J.; Pietron, J. J.; Murray, R. W.; Schaff, T. G.; Khoury, J. T.; Alvarez, M. M.; Whetten, R. L. *Science* **1998**; 280; 2098.

(10) Chen, S.; Murray, R. W.; Feldberg, S.; *J. Phys. Chem.* **1998**; 102; 9898.

(11) Chen, S.; Murray, R. W.; *Langmuir* **1999**; 3; 682.

(12) Hicks, J. F.; Templeton, A. C.; Chen, S.; Sheran, K. M.; Jasti, R.; Murray, R. W.; *Anal. Chem.* **1999**; 71; 3703.

(13) Song, Y.; Jimenez, V.; McKinney, C.; Donkers, R.; Murray, R. W. *Anal. Chem.* **2003**, *75*, 5088.

(14) Jimenez, V. L.; Leopold, M. C.; Mazzitelli, C.; Jorgenson, J. W.; Murray, R. W. *Anal. Chem.* **2003**, *75*, 199.

(15)   Song, Y.; Heien, M. LAV; Jimenez, V.; Wightman, R. M.; Murray, R. W. *Anal. Chem.* **2004**, *76*, 4911.

(16)   Wei, G.-T.; Liu, F.-K.; Wang, C. C. R. *Anal. Chem.* **1999**, *71*, 2085.

(17)   Wei, G.-T.; Liu, F.-K. *J. Chromatogr., A* **1999**, *836*, 253.

(18)   Novak, J. P.; Nickerson, C.; Frqanzen, S.; Feldheim, D. L.; *Anal. Chem.* **2001**; 73, 5758.

(19)   Choi, M.; Douglas, A. D.; Murray, R. W.; *Anal. Chem.* **2006**; 78; 2779.

(20)   Schaaff, T. G.; Whetten, R. L. *J. Phys. Chem. B* **2000**, *104*, 2630.

(21)   Negishi, U.; Nobusada, K.; Tsukuda, T. *J. Am. Chem. Soc.* **2005**, *127*, 5261.

(22)   Templeton, A. C.; Cliffel, D. E.; Murray, R. W. *J. Am. Chem. Soc.* **1999**, *121*, 7081.

(23)   Rodriguez, M. A.; Armstrong, D. W. *J. Chromatogr., B* **2004**, *800*, 7.

(24)   Liu, F.-K.; Lin, Y.-Y.; Wu, C.-H. *Anal. Chim. Acta* **2005**, *528*, 249.

(25)   Hostetler, J. H.; Templeton, A. C.; Murray, R. W.; *Langmuir* **1999**; 15; 3782.

(26)   Song, Y.; Murray, R. W.; *J. Am. Chem. Soc.* **2002**. 124; 7096.

(27)   Song, Y.; Huang, T.; Murray, R. W.; *J. Am. Chem. Soc.* **2003**. 125; 11694.

(28)   Donkers, R. L.; Song, Y.; Murray, R. W.; *Langmuir* **2004**. 20; 4703.

(29)   Guo, R.; Song, Y.; Wang, G.; Murray, R. W.; *J. Am. Chem. Soc.* **2005**; 124; 2752.

(30)   Templeton, A. C.; Hostetler, M. J.; Warmoth, E. K.; Chen, S.; Hartshorn, C. M.; Krishnamurthy, V. M.; Forbes, M. D. E.; Murray, R. W.; *J. Am. Chem. Soc.* **1998**. 120; 4845.

(31)   Tognarelli, R. B. M.; Pompano, R. R.; Loftus, A. F.; Sheibley, D. J.; Leopold, M. C.; *Langmuir*; **2005**. 21; 11119.

(32)   Sheibley, D.; Tognarelli, R. S.; Leopold, M. C.; *J. Mater. Chem.* **2005**. 15; 491.

(33)   Shenhar, R.; Rotello, V. M; *Acc. Chem. Res.* **2003**. 36, 549

(34)   DeVries, G. A.; Brunnbauer, M.; Hu, Y.; Jackson, A. M.; Long, B.; Neltner, B. T.; Uzun, O.; Wunsch, B. H.; Stellacci, F.; *Science* **2007**; 315; 358.

(35)   Novak, J. P.; Feldheim, D. L.; *J. Am. Chem. Soc.* **2000**; 122; 3979

(36)   Novak, J. P.; Brousseau, L. C.; Vance, F. W.; Johnson, R. C.; Lemon, B. I.; Hupp, J. T.; Feldheim, D. L.; *J. Am. Chem. Soc.* **2000**; 122; 12029.

(37)   Schaaff, T. G.; Whetten, R. L.; *J. Phys. Chem. B* **2000**, *104*, 2630.

(38)   Negishi, Y.; Takasugi, Y.; Sato, S.; Yao, H.; Kimura, K.; Tsukuda, T.; *J. Am. Chem. Soc.* **2004**, *126*, 6518.

(39)   Tracy, J. B.; Kalyuzhny, G.; Crowe, M. C.; Balasubramanian, R.; Choi, J.-P.; Murray, R. W. *J. Am. Chem. Soc.* **2007**, *129*, 6706.

(40)   Tracy, J. B.; Crowe, M. C.; Parker, J. F.; Hampe, O.; Fields-Zinna, C. A.; Dass, A.; Murray, R. W. *J. Am. Chem. Soc.* **2007**, *129*, 16209.

(41)   Dass, A.; Stevenson, A.; Dubay, G. R.; Tracy, J. B.; Murray, R. W. *J. Am. Chem. Soc.* **2008**; 130(18); 5940.

(42)   Heaven, M. W.; Dass, A.; White, P. S.; Holt, K. M.; Murray, R. W. *J. Am. Chem. Soc.* **2008**, *130*, 3754.

(43)   Akola, J.; Walter, M.; Whetten, R. L.; Häkkinen, H.; Grönbeck, H. *J. Am. Chem. Soc.* **2008**, *130*, 3756.

(44)   Zhu, M.; Aikens, C. M.; Hollander, F. J.; Schatz, G. C.; Jin, R. *J. Am. Chem. Soc.* **2008**, *130*, 5883.

(45)   Chaki, N. K.; Negishi, Y.; Tsunoyama, H.; Shichibu, Y.; Tsukuda, T. J. Am. Chem. Soc.; **2008**; 130(27); 8608.

(46)   Brust, M; Walker, M.; Bethell, D.; Schriffrin, D. J.; Whyman, R. *J. Chem. Soc. Chem. Commun.* **1994**, 801.